Impact of iron oxide nanoparticles on a lead polluted water-soil-plant system under alternating periods of water stress

Léa Mounier, Mathieu Pédrot, Martine Bouhnik-Le-Coz, Francisco Cabello Hurtado

Environmental Science Advances

Accepted Manuscript

This article can be cited before page numbers have been issued, to do this please use: L. Mounier, M. Pédrot, M. Bouhnik-Le-Coz and F. Cabello Hurtado, *Environ. Sci.: Adv.*, 2023, DOI: 10.1039/D2VA00283C.

ROYAL SOCIETY OF CHEMISTRY

rsc.li/esadvances

Impact of iron oxide nanoparticles on a lead polluted water-soil-plant system under alternating periods of water stress

Léa Mounier[a,b], Mathieu Pédrot[b], Martine Bouhnik-Le-Coz[b], Francisco Cabello Hurtado[a*]

[a]Univ Rennes 1, CNRS, ECOBIO, UMR 6553, Av. General Leclerc, F-35042 Rennes Cedex, France.

[b]Univ Rennes 1, CNRS, Géosciences Rennes, UMR 6118, Av. General Leclerc, F-35042 Rennes Cedex, France.

* Corresponding author. Phone: +33 2 23235022. Email: francisco.cabello-hurtado@univ-rennes1.fr

Environmental significance

Many sites are contaminated with lead for which several types of remediation systems have been tested. Phytoremediation is one of these methods, environmentally friendly but slow, which we tried to improve with the addition of iron oxide nanoparticles. Indeed, magnetite nanoparticles, known for their high sorption capacity, can be used to act on Pb dynamics. This long-term study investigated the potential of magnetite nanoparticles for lead remediation in a complete cultivation system including water, soil and plant compartments. Influencing Pb mobility and impacting both soil, leached soil solution and plants, the findings result shows that magnetite nanoparticles are promising materials for trace elements phytoremediation and plant stress tolerance, allowing to associate a decrease of Pb mobility in leachates while increasing its bioavailability.

Abstract

Iron oxide nanoparticles (IONPs) are a promising material for the remediation of trace elements which are a significant source of soil pollution. Thus, as part of improving phytoremediation processes, the addition of IONPs to soil was tested in this study. A long-term experiment was performed in pot to assess the potential of magnetite (Fe_3O_4)

nanoparticles (NPsMagn) to modify lead (Pb) availability to sunflower (*Helianthus annuus*) and its behavior in a water-soil-plant system under repeated water-deficiency stress. Plants were grown either in control soil, Pb polluted soil (final added lead 375 mg kg^{-1}), Pb polluted soil containing 1 % dry weight NPsMagn or Pb polluted soil containing 1 % dry weight micro-sized magnetite for 90 days. Pb polluted soil and Pb treated soil containing NPsMagn do not affect plant growth but NPsMagn allow reduced oxidative impact as a decrease in lipid peroxidation was observed in their presence. Magnetic susceptibility measurements and Fe content in sunflower plants and leachates suggest that NPsMagn penetrate the roots but are not dispersed in soil solution. In addition, Pb content increased by 102 % and 22 % respectively in leaves and stems of plants treated with NPsMagn. Based on Pb content in soil solutions, NPsMagn decrease Pb in leachate by 50 %. During water stress periods, NPsMagn significantly improve water retention in soil and relative water content in plants. As a result of this, NPsMagn improve Pb availability and accumulation in sunflower plants in TEs contaminated soils unfavorable to plant growth. This study also highlights favorable effects of NPsMagn on Pb stabilization into soil, reducing their loss in leachates and on plant tolerance during water stress periods.

Key words: magnetite nanoparticles, sunflower, lead pollution, phytoremediation, water stress

1. Introduction

Due to human activities, trace element (TE) pollution has become widespread and constitutes a threat to the environment and human health. Several million tons of TEs have been released into the environment during the last century,[1] spreading TEs at the worldwide level even in remote ecosystems.[2] Among these TEs, lead (Pb), mainly resulting from mining production, industries and transport, is one of the ubiquitously distributed most abundant toxic elements in soil and water without biological function.[3] In the last decades, an estimated 783,000 tons of Pb have been dispersed in the environment worldwide.[1]

Through its bioaccumulation and nonbiodegradability, Pb soil contamination may cause significant hazard to human being, animals and plants.[4] Lead has a strong effect on plants because it may impact all aspects of plant growth and health even at very low Pb concentration.[5] Plant germination has been shown to be inhibited [6] and biomass production of roots and aerial parts may also be affected up to half.[6–8] Furthermore, Pb also impacts the

View Article Online
DOI: 10.1039/D2VA00283C

metabolism of plants (e.g. decreasing photosynthetic activity, protein content, nutrient uptake, respiration rate and ATP content; or increasing lipid peroxidation and oxidative stress).[9] ROS production caused by Pb toxicity may led to oxidative stress, which is widely identified as an indicator of plant stress and may lead to cell death.[10,11] In some cases, Pb and TEs in general can be translocated from plants to the human dietary system posing a major threat to human health.[12] Therefore, it has become necessary to take proactive measures to detoxify the Pb-polluted soils.

Nanotechnology is an emerging field that covers a wide range of technologies currently being developed at the nanoscale. Among them, environmental nanotechnologies have enormous potential to provide innovative solutions to a wide range of environmental problems. These include improved methods for pollution abatement, water treatment, environmental sensing and remediation, and making alternative energy sources more cost-effective. The unique properties (e.g. small size, high surface area) of engineered nanomaterials enable these new technologies to address environmental challenges in a sustainable manner. The main objective of environmental nanotechnology also includes the safe design of nanomaterials with potential environmental benefits and the promotion of sustainable development of these materials.[14,15] NPs such as iron oxide nanoparticles (IONPs) can interact with pollutants in soils and soil solutions, such as heavy metals, pesticides or other contaminants, and are promising materials for the stabilization of TEs.[16] For instance, IONPs has been applied for scavenging pollutants such as nitrate,[17] antibiotic medication,[18] or TEs such as Cr(VI),[19] Cd(II),[20] As(V),[21] Se (IV),[22] and Pb(II)[23] from the aqueous media. Due to their high surface area, which promotes an elevated sorption capacity, IONPs can impact mobility, availability and toxicity of TEs and in particular they limit the transport of Pb and the contamination of groundwater in case Pb is neither absorbed by roots nor by soil particles.[24] Thus, IONPs effectively scavenge TEs and limit their transport through chemical mechanisms involving adsorption (both physical and chemical),[25,26] incorporation, and electron transfer (e.g. reduction of As(V) to As(III)[27]) .[28] For instance, Demangeat *et al.* observed that increased Cu adsorption into IONPs was related to pH augmentation, which caused decreasing protons concentration at magnetite surface favoring cation attraction.[29] Under certain conditions, IONPs have been shown to decrease the toxicity of some TEs by decreasing their availability to plants.[30] An amendment of IONPs

View Article Online
DOI: 10.1039/D2VA00283C

significantly reduced soluble Zn in the soil solution by 22 %, demonstrating that IONPs acted by fixing Zn in the soil.[30]

In addition, the presence of IONPs could both influence the absorption and accumulation of TEs in plants, as well as enhance plant growth through improved nutrition and fertilization.[28,31] Studies showed that NPs could enhance the plant capacity to absorb more nutrients and increase efficiency of NPK use.[32] Also, organic matter (OM) can bound with IONPs (e.g. through hydrogen bounding, cation bridges and van der Waals interactions) and thus IONPs increase OM amount due to its high surface area.[16] Iron availability for plant growth is also under control of Fe solubilization from iron-rich minerals. This nutrient exchange is mediated by chemicals (pH and dissolution-precipitation) and biological (e.g. roots exudates release) processes. Even if it has been demonstrated that IONPs have limited penetration into plants, they aggregate onto roots surface.[33] Accumulation of IONPs on roots could allow to increase bioaccumulation of associated Pb. However, the processes underlying NP-mediated TEs uptake and toxicity reduction vary with NPs type, mode of application, time of exposure and plant conditions (e.g. species, varieties, and development rate).[14] Current researches are testing the use of IONPs to reduce the phytotoxicity caused by toxic TEs[34–36] and improve plant growth.[36,37]

Thus, IONPs might be used in combination with plants for remediating soils contaminated by TEs but, to take advantage of the potential of IONPs for remediation, issues concerning IONPs availability, biocompatibility and behavior in soil and soil solution need to be further investigated. Sunflower (*Helianthus annuus*) was selected for the current study as it has a high biomass production and has a promising phytoremediation potential due to its high ability to adsorb, stabilize and accumulate different concentrations of Pb[40] as well as a tolerance to periods of water stress.[41] In this context, the objectives of the experiment were to (i) study the impact of both IONPs and Pb concerning their behavior in a water-soil-plant system, (ii) assess Pb phytoextraction potential by sunflower treated with IONPs, (iii) evaluate the plant-protection capacities of IONPs under Pb pollution.

2. Materials and methods

View Article Online
DOI: 10.1039/D2VA00283C

2.1. Synthesis and characterization of iron oxide nanoparticles

Iron oxide nanoparticles, namely magnetite (Fe_3O_4) nanoparticles (NPsMagn), have been synthesized following co-precipitation method[42,43] in aerobic condition, and presented size and surface area as in Demangeat *et al*.[29] A solution of $FeCl_2$ and $FeCl_3$ (1:2 molar ratio) was mixed into NaOH solution leading to precipitation of magnetite particles, and solid phases were washed with ultrapure water. The final solution consisted of a non-stoichiometric magnetite $Fe_{3-\delta}O_4$ with a Fe_{II}/Fe_{III} ratio between 0.15 and 0.1 determined by spectrophotometric method as described by Jungcharoen *et al*.[44] The size, shape, surface area and pH_{zpc} of NPsMagn were determined according to the methods described in Demangeat *et al.*[29] Thus, the synthesized NPsMagn have a round crystalline shape of 9±2 nm diameter (ESI Fig. S1) with a specific surface area and pH_{zpc} respectively established at 115 $m^2\ g^{-1}$ and 6.2. A micrometer-sized magnetite (particles < 5µm) (µMagn) solution was prepared by diluting magnetite (310069 Sigma-Aldrich) in ultrapure water to the desired concentration.

2.2. Experimental design

A 90-day culture was performed with sunflower (*Helianthus annuus*) plants. The experimental set-up consisted of two nested pots (400 mL polypropylene beaker, Nalgene). The top pot contains the soil (335 g dry weight (DW) per pot) and a nylon cloth (31 µm diameter) was added to the bottom of the top pot to hold the soil particles in the higher part of the system. The top pot was pierced to allow soil solution to run out and be collected in a second pot (ESI Fig. S2). The soil used was collected on grove-type site between the 10 to 20 cm-deep first horizon, homogenized and sieved to 5 mm diameter. Soil characterization was carried out (ESI Tab S1) and the initial content in Pb determined (53.8 mg kg^{-1} DW).

Four treatments of six replicates have been constituted for plant cultivation: unmodified soil (Control), soil polluted with added Pb (Pb), soil polluted with added Pb and containing 1 % NPsMagn (NPsMagn-Pb) and soil polluted with added Pb and containing 1 % of micrometer-sized magnetite (µMagn-Pb). In addition, Pb and NPsMagn-Pb treatments (three replicates each) have also been studied without plants (Soil Pb and Soil NPsMagn-Pb, respectively). The soil has been initially contaminated with added lead at a concentration of 150 mg kg^{-1} of dry soil by adding 50 mL per pot of 4.85 mM $Pb(NO_3)_2$ into pristine soil and homogenized. This concentration is above toxicity threshold set in France[45] and corresponds to the toxicity limit

View Article Online
DOI: 10.1039/D2VA00283C

in *H.annuus* found in literature.[7] Three new additions of $Pb(NO_3)_2$ corresponding to 75 mg Pb per kg soil each (at days 35, 42 and 49) brought the final added lead concentration to 375 mg kg^{-1} soil. NPsMagn solution (23 g L^{-1}) has been added to achieve 1 % (m/m) of dry soil to provide a consistent amount of material to achieve an optimal removal of TEs in soil according to Komárek *et al.*[24] Likewise, micrometer-sized magnetite solution (25 g L^{-1}) has been added into soil up to 1 % (m/m) of dry soil and homogenized.

Sunflower seeds were washed 3 minutes in a 3 % sodium hypochlorite bath and then rinsed five times during 12 minutes in distilled water baths. Seeds were first sown into pristine soil and placed in a climatic chamber. After 18 days of growth, young plants with the same state of growth were transplanted in experimental set-up. Cyclic growth parameters of climatic chamber allowed 16 h light at 21 °C and 8 h dark at 18 °C, a photosynthetic photon flux density of 160 µmol m^{-2} s^{-1}, and a relative humidity of 70 %.

Each week, soils were kept at field capacity with 0.5 mM NaCl solution during 4 days, followed by a period of 3 days of water deficit (absence of irrigation). Once a week, soil solution has been harvested by increasing the watering. For pots cultivated with plants, soil solutions collected from the six replicates were mixed two by two and homogenized at each sampling allowing to obtain a sufficient volume so that three samples per treatment were generated for geochemical analyses. In the case of the soil solutions of non-cultivated pots, two samples were generated by dividing soil solution of the second pot in two halves and then each half was homogenized with soil solution of pots 1 and 3 respectively.

After 90 days of culture, plants were harvested for biological analyses. Pictures were taken, and the fresh weights of roots, leaves and stem were measured for each individual (if flower buds were present they were counted with the leaves). Samples were frozen in liquid nitrogen and stored at -80°C. For NPsMagn-Pb treatment, roots and stem/leaves have been vertically divided into three parts of equal length to assess the presence of NPsMagn into plants thanks to magnetic susceptibility measurement. Soil for each replicate was also collected and separated in three equal vertical parts for the purpose of magnetic susceptibility measurements. For aerials parts, the 3 sections were named from bottom to top: “L1” (lower third), “L2” (mid third) and “L3” (upper third) for leaves (T1, T2 and T3 for stem). Similarly, roots (R1, R2 and R3) and soil (S1, S2, S3) parts were numbered from 1 to 3 with increasing depth.

View Article Online
DOI: 10.1039/D2VA00283C

2.3. Biological assays

In order to perform biological analyses, plant samples were first dried by lyophilization (Christ ALPHA 1-2LDplus) and then grinded by mill (Mixer Mill MM400). Frozen samples were placed into the chamber for a primary long drying (0.09 Pa for 72h), followed by a secondary short drying stage (0.001 Pa for 24h). Dried vegetative samples were grinded using zirconium bowls and beads.

2.3.1. Pigment content

To determine chlorophyll and carotenoid contents, 5 mg DW of *H.annuus* leaves were added to 500 µL of acetone 80 %, mixed 10 min at 4 °C and incubated in the dark 12 h at 4 °C. After complete bleaching, samples were centrifuged at 12 000 *g*. Supernatants were recovered in new tubes, and 30 µL of each were diluted in 270 µL acetone (80 %) in microplate wells. Pigment content was measured by spectrophotometrically reading the absorbance at 470, 645 and 663 nm (spectrometer SAFAS FLX-Xenius). Pigment content was then determined based on the equations of Lichtenthaler and Wellburn (1983).[46]

2.3.2. Amino acid content

To determine amino acid content, total amino acids were first extracted with 30 mg dried leaves added with 1 mL ethanol (100 %) and heated at 95 °C for 10 min with opened caps to allow ethanol to evaporate, and then added with 1 mL ultra-pure water and centrifuged at 10 000 *g* for 10 min at 4°C. Supernatants were collected and stored at -20 °C.

Determination of total amino acids was performed following Yemm *et al.* method,[47] improved by Magné and Larher.[48] 100 µL of amino acids extract were added with 0.5 mL citrate buffer (177 mM, pH 4.6 containing 300 mM sodium hydroxide) and 1 mL of ninhydrin solution (47 mM ninhydrin, 50 mM ascorbic acid, ethanol (70 % v/v)) and heated at 95 °C for 20 min. 3 mL ethanol (70 %) were added and absorbance at 570 nm was measured by spectrophotometry in glass tank. Leucine was used to determine the amino acid contents (calibration solution range from 0 to 10 mM).

Determination of proline content was performed following Troll and Lindsley method.[49] 100 µL of amino acids extract were added with 1 mL of ninhydrin solution (6 mM ninhydrin, acetic acid (60 % v/v)) and heated at 95 °C for 20 min. Samples were cooled in water for 15 min,

View Article Online
DOI: 10.1039/D2VA00283C

added with 3 mL of toluene and placed 1 h in the dark. After phase separation, the top solutions were slightly poured into a glass tank and absorbance was measured at 520 nm.

2.3.3. Determination of lipid peroxidation

Quantification of lipid peroxidation products is achieved by measurement of thiobarbituric acid reactant species (TBARS) according to the corrected method proposed by Hodges *et al*.[50] 15 mg dried leaves were added with 1 mL ethanol (80 %) and let react for 25 min in a rotation wheel at room temperature. After centrifugation for 10 min at 10 000 *g*, supernatants were collected in new tubes. Two aliquots of 200 µL were prepared and added with 200 µL of TBA+ solution (20 % (w/v) trichloroacetic acid, 0.65 % (w/v) TBA and 0.01 % (w/v) butylhydroxytoluene). Two others aliquots were mixed with TBA- solution (20 % (w/v) trichloroacetic acid, 0.01 % (w/v) butylhydroxytoluene). Samples were heated at 95 °C for 25 min then centrifuged for 10 min at 10 000 *g* after cooling at room temperature. Supernatants were recovered in new tubes, and 300 µL were placed in microplate wells. Supernatant absorbance was measured at 440, 532 and 600 nm (spectrometer SAFAS FLX-Xenius) and results were expressed in malondialdehyde equivalents (MDAeq) per gram of plant DW according to Hodges *et al.* [50] equations.

2.3.4. Soluble protein extraction and quantification

For soluble protein extraction, 50 mg dry leaves were added to 1.5 mL sodium phosphate buffer (50 mM, pH 7.5) containing 1 mM Na-EDTA, 5 % (w/v) Polyvinylpyrrolidone, 0.5 % (v/v) protease inhibitor cocktail (Sigma-P9599) and 0.1 % (w/v) Triton X-100. Samples were shaken during 1 h at 4 °C, then centrifuged twice at 12 000 *g* for 12 min and supernatants were collected in new tubes. Soluble protein quantification was performed according to Bradford's method by spectrophotometric determination.[51] Bovine serum albumin (BSA) was used to determine the protein contents (calibration solution range from 0.1 to 1.4 mg L^{-1}). Protein extracts were kept at -80 °C until used for POD and SOD enzymatic antioxidant activity assays.

2.3.5. Determination of POD activity

Guaiacol peroxidase (POD) activity was determined based on some modified literature.[52] Reaction occurs in microplate well where reaction mixture consists of 190 µL deionized ultrapure water, 30 µL potassium phosphate buffer (1 M, pH 6.5), 30 µL guaiacol (150 mM) and 50 µL soluble protein extract. Reaction was triggered by addition of 30 µL of H_2O_2 (160

View Article Online
DOI: 10.1039/D2VA00283C

mM) and monitored by reading absorbance at 470 nm ($\varepsilon_{tetraguaiacol}$= 26.6 mM^{-1} cm^{-1}) for 6 min. The observed increase in absorbance provided the maximum rate of tetraguaiacol formation and was used to determine the enzymatic activity. The amount of enzyme that reduced 1 mmol of H_2O_2 per min corresponds to 1 unit (U) of POD under the assayed conditions.

2.3.6. Determination of SOD activity

The capacity of superoxide dismutase (SOD) to inhibit the photochemical reduction of nitro blue tetrazolium (NBT) was measured following the modified method of Giannopolitis and Ries.[53] Each microplate well was filled with 175 µL deionized ultrapure water, 30 µL potassium phosphate buffer (500mM, pH 7.8), 30 µL of methionine (130 mM), 30 µL of NBT (750 µM) and 5 µL of soluble protein extract. Two microplates were prepared, one exposed to light and one kept in the dark (for light-independent reactions corrections) for spectrometric analysis. A pre-reading of each plate was realized at 560 nm before initiating the reaction. Then, 30 µL of riboflavin (20 µM) was added in each well to start the reaction and samples were exposed either to light (30 min) or kept in the dark. The absorbance was measured at 560 nm, and pre-read values were subtracted from the final absorbance measurement. SOD activity has been expressed in U mg^{-1} protein, "U" corresponding to the amount of enzyme causing 50 % inhibition of the NBT reduction to blue formazan observed in the absence of the enzyme.

2.4. Leaf angle measurement

Photos used for the measurement of leaf angle were taken twice a week at the beginning and the end of water stress periods. Leaf inclination angle was measured using the ImageJ software and corresponds to the angle between the abaxial face of the leaf and the petiole (measurements were made on four leaves per plant).

2.5. Relative water content

To determine relative water content (RWC), 10 leaf discs (1 cm diameter) were collected and fresh weights (FW) were measured. Leaf discs were immersed for 24 h in distilled water and then turgescent weights (TW) were assessed. Leaf discs were heated at 70 °C for 48 h and the DW were determined. The RWC was evaluated following the equation: RWC= ((FW-DW)/ (TW-DW)) × 100.

2.6. Geochemical analyses

View Article Online
DOI: 10.1039/D2VA00283C

The pH was measured with a combined Mettler InLab electrode after a calibration performed with 3 standard buffers (pH 4, 7, and 10). The redox potential was measured with a Pt electrode combined with a Ag/AgCl reference electrode (Fisher Scientific Bioblock). The Eh values are presented in millivolts relative to the standard hydrogen electrode, including a correction measurement using a commercial redox buffer (220 mV vs Ag/AgCl). Soil solutions have been filtered at 0.2 µm with syringe filters to remove particles. 10 mL of the filtered soil solutions were directly acidified by subboiled nitric acid (HNO_3; 14.6 N) at 2 % v/v for ICP-MS analysis, the remainder were placed at 4 °C.

2.6.1. Trace elements measurements

Lead and iron concentrations were determined by ICP-MS (Agilent 7700x) using rhenium and rhodium as internal standards. The international geostandard SLRS-6 was used to check the validity and reproducibility of the results. Typical uncertainties including all error sources were below ± 5 % for Fe and Pb. Samples were prepared in clean room and tubes were pre-washed (24 h in 1.5 M HNO_3 at 45 °C, 24 h in deionized ultrapure water at 45 °C).

For biological samples, 100 mg plant DW were added with 5 mL 14.6 N subboiled HNO_3, 1 mL 37 % H_2O_2 and 1 mL ultrapure water in specific digestion tubes (Anton Paar Teflon 18 mL vials). Samples were digested using a multiwave (Multiwave 7000 Anton Paar) using a specific program. First step consists of increasing temperature to 250 °C for 20 min at 140 bars, then temperature is kept at 250 °C for 30 min at 140 bars. Next, the digested solutions were transferred into digestion vessels (Savillex Teflon vials) and were heated until evaporation of the solvent. Samples were solubilized in 0.37 M subboiled HNO_3 with appropriate dilution(s) considering ICP-MS quantification limits.

2.6.2. Determination of dissolved organic carbon

Amount of dissolved organic carbon (DOC) was determined with a Total Organic Carbon Analyzer (TOC-L SHIMADZU). The accuracy of DOC measurement was estimated at ± 3 % (respectively by using standard solution of potassium hydrogen phthalate).

2.6.3. Determination of soil water potential

The soil water potential was determined by a WP4C dew point meter (METER Group, Inc). The measurements were performed on soil taken after plant harvest in each treatment. Same

View Article Online
DOI: 10.1039/D2VA00283C

amount of soil was filled in the WP4C sample cup and placed in the block chamber of WP4C for measurement.

2.7. Magnetic susceptibility measurements

In order to evidence magnetite presence in environment, magnetic susceptibility has already been used.[54] Here magnetic susceptibility measurements were conducted to track and quantify NPsMagn in different parts of sunflower plants and in soil. Analyses were performed with a magnetic susceptibility meter (Kappabridge AGICO KLY3).

To perform the measurements, samples were dried by lyophilization and stored in clean plastic containers. To account for the container signal, blanks (containers without samples) were used at the beginning and end of the acquisitions and after every 10 measurements. To ensure the validity and reproducibility of the results, magnetic susceptibility measurements were repeated 12 times for each sample. Then mass susceptibilities ($m^3\ kg^{-1}$) were calculated considering samples weight. From these values, NPsMagn concentration into the samples was determined based on the blank-corrected magnetic susceptibility of a sample of NPsMagn of known weight.

2.8. Statistical analysis

Each value is presented as the mean ± standard error of the mean (SEM), with at least 3 replicates. Normality was confirmed with Shapiro test and homoscedasticity with Bartlett test for each assay. Statistical analyses were conducted using the Tukey test (ANOVA) or Kruskall Wallis test to assess the significance of the means taking $p<0.05$ as significant. Data significantly different are indicated with different letters.

3. Results and discussion

3.1. Physiological and biochemical responses of *Helianthus annuus* plants exposed to NPsMagn in a Pb pollution context

3.1.1. Growth parameters

After 90 days of plant growth, no significant difference was observed for either leaves or stems dry weight (Fig. 1) and plant height (averaged 55 cm, data not shown) between control plants and plants submitted to any of the treatments.

View Article Online
DOI: 10.1039/D2VA00283C

Even if NPsMagn-Pb treatment did not promote a significant increase in aerial biomass, our results show the harmlessness of a NPsMagn treatment at remediation concentrations (1 %)[24] in Pb-polluted soils, which is in agreement with recent research in our laboratory concerning NPsMagn impact on sunflower plants under Cu pollution.[54] Although, it is possible that the action of NPsMagn has been affected by different factors such as the application concentration, the plant species, duration of the experiment, the culture medium, or the plant development stage.[55] It can also be nuanced that the size of the experimental set-up used may have been a limiting factor in plant development, as sunflowers can reach much greater heights and biomass in environment. In the present study, even if the 1 % NPsMagn did not impact the growth, the initiation of flower buds could be affected because buds were present in all the plants exposed to NPsMagn-Pb and they were more developed than in the others treatments after 90 days of growth. Indeed, no flower buds were observed for control treatment, and only one and two flower buds out of six plants respectively in µMagn-Pb and Pb. In contrast with these results, previous work[54] showed a delay in flowering of sunflowers treated with NPsMagn and no flowering at all for sunflowers germinated and grown with NPsMagn under Cu pollution. However, in this study[54] the seeds were put to germinate directly in contact with the various treatments which could have caused a global growth delay in the case of NPsMagn treatments.

Furthermore, here the presence of Pb in the soil at a final added concentration of 375 mg kg^{-1} soil did not impact leaves or stem biomass production, which is in contrast to what can be found in literature.[7,56] However, Madejón *et al.* showed a different impact of TEs, including Pb, on the growth of sunflower according to the stage of development of the plant.[57] Soil pollution significantly retarded early growth of youngest plant (1 month after sowing), especially root growth. In our experimental set-up, even if only an estimate of root biomass was made because the whole roots could not be precisely and equally recovered from the soil (ESI Fig. S3), visual observation provided a sufficient bases to note that root growth was impacted by Pb pollution. On the contrary, Madejón *et al.* found no differences in sunflower biomass production after 130 days of growth in Pb contaminated soil (113 mg kg^{-1}) compared to control.[57] As we introduced 18-day-old seedlings into the experimental set-up, it is likely that aerial parts were not impacted by Pb because they had already passed this critical growth period.

View Article Online
DOI: 10.1039/D2VA00283C

3.1.2. Pigment contents

For each condition, contents of chlorophylls (*Ca* and *Cb*) and carotenoids (*K*) follow the same pattern (Fig. 2). As for plant growth parameters, the leaves of plants exposed to Pb contain similar pigment levels than control. The highest content is found after µMagn-Pb treatment, under which the pigment contents are roughly one third higher than in the control. Reversely, the pigment contents are significantly lower in NPsMagn-Pb than in Pb and µMagn-Pb treatments (Fig. 2), and *Ca/Cb* ratio decreased by 11% in NPsMagn-Pb compared to control leaves (Fig. 2). However, in spite of these differences in pigment contents, none of the treatments affected the maximum quantum yield of photosynthesis (ESI Tab S2).

Several studies reported that IONPs can affect pigment concentrations of exposed plants.[58] Thus, to mention only sunflower, a previous work found that NPsMagn diminished chlorophyll and carotenoid contents up to 50 % in sunflower seedlings and the combination with Pb could contribute to increase this impact.[59] Otherwise, IONPs can induce no effect[60] or increase[61] pigment contents.

It has also been documented that photosynthesis inhibition is a symptom of Pb toxicity due to several Pb effects varying according to plant species: inhibition of chlorophyll and carotenoid synthesis, distorted chloroplast ultrastructure, obstruction of the electron transport system, inhibition of Calvin cycle enzymatic catalysis, impaired uptake of essential elements such as Mn and Fe and substitution of divalent cations by Pb, or increased chlorophyllase activity.[9] Nevertheless, this impact is affected by Pb doses in combination with soil properties as will be discuss later (section 3.2.2).

3.1.3. Concentrations of total free amino acids

The amount of total free amino acids is equivalent among treatments (6 µg g^{-1} DW), except for NPsMagn-Pb which total free amino acids is higher by 50 % (Fig. 4). As Pb alone seems to have no impact on sunflowers amino acid content (Fig. 4), it is likely that NPsMagn have an effect on primary metabolites production. Zahra *et al.*[62] have reported that the external addition of NPs can change the level of most amino acids in plants. They observed that the use of TiO_2 NPs in wheat induced an increase in amino acid production. The cessation of sugar biosynthesis, due to the disruption of photosynthesis, shifted the cellular metabolism to the

View Article Online
DOI: 10.1039/D2VA00283C

use of amino acids as an alternative energy source.[63] Also, Fe_2O_3 NPs induced an increase in cysteine and tyrosine content in wheat.[64]

3.1.4. Oxidative stress response

TBARS (like malondialdehyde, MDA) are the result of the decomposition of unstable and reactive lipid peroxides produced by lipid peroxidation that occurs in cells after an oxidative stress.[50] As the TBARS content reflects the degree of oxidative injury to a plant cell, the decreased TBARS content is inferred to result from the absence of oxidative injury from the treatment applied. TBARS content in NPsMagn-Pb is similar to control, while this amount is significantly higher by 21 % in Pb and µMagn-Pb treatment (Fig. 3A). Thus, NPsMagn likely provide or induce a protection against lipid peroxidation caused by lead treatment, which was not observed for µMagn. Demangeat *et al.*[54] showed a similar pattern of lipid peroxidation reduction in sunflower plants when they were exposed to NPsMagn or NPsMagn-Cu compared to Cu treatment. This protective effect of IONPs against lipid peroxidation has also been demonstrated for other plant species.[37,65]

POD and SOD are part of the enzymes that participate in protection mechanisms against oxidative damage. We did not observe significant differences in POD or SOD activities between treatments, except for POD activity in Pb treated plants which is twice higher than in the control group (Fig. 3B, 3C). Increasing the activities of SOD and POD has been shown to provide better mechanisms for protecting plants from oxidative damage.[66] In particular, POD, by catalyzing the reaction between H_2O_2 and ROOH to H_2O and R-OH, directly protects against cellular damage.[67] In their study, Demangeat *et al.*[54] showed a correlation between TBARS content decreased and antioxidant POD activity increased in NPsMagn-Cu treated plants, suggesting that POD antioxidant response acted effectively against ROS under Cu exposition. In our study, the lower POD and TBARS contents seem to indicate less oxidative stress in the plants under the NPsMagn-Pb treatment, underlining the protective effect of NPsMagn. Interestingly, as already mentioned, amino acid content is higher in NPsMagn-Pb treated plants (Fig. 4). It has been shown that under stress conditions, abundant amino acids are synthesized to help plant to cope with stress provoked imbalances.[68] On the other hand, the two-fold increase in POD and TBARS content in the Pb treatment suggests that plant cells probably accumulate more ROS in response to Pb pollution, which causes lipid peroxidation of membranes and induces antioxidant mechanisms to cope with.

View Article Online
DOI: 10.1039/D2VA00283C

3.2. Fate of NPsMagn and Pb in a water-soil-plant system

3.2.1. Uptake and translocation of NPsMagn from soil to plant

Iron was mainly found in the leaves where iron levels varied from 34 mg kg^{-1} DW (Control) to 38 mg kg^{-1} DW (NPsMagn-Pb) but no significant differences in Fe content in sunflower leaves were observed between treatments (Fig. 5A). Even if Fe content in the stems is, regardless of the treatment, lower than in the leaves, it is significantly higher by 23 % in stems of plants treated with NPsMagn-Pb compared to Control (Fig. 5A). On the contrary, stem Fe content significantly decreased by 18 % in µMagn-Pb condition compared to control.

Concerning the fate of NPsMagn in soil, no significant differences between treatments are found in magnetic susceptibility measurements in soil, suggesting that NPsMagn did not migrate over times with leachates (Tab 1). NPsMagn tend to aggregate to mm-sized particles and such tendency to aggregate may result in decreased NPsMagn mobility in soil,[69] as does the bonding of NPsMagn to clays and organic matter (OM) in the soil because of their high affinity for each other.[69]

Previous studies in the literature have reported that NPs accumulated primarily at the root level, before entering the upper parts of the plant.[33] Here, based on magnetic susceptibility measurements, NPsMagn were detected in the roots but not in aerial parts of sunflower plants grown in NPsMagn-Pb contaminated soil. NPsMagn content in roots significantly decreases from top to bottom of the roots (Tab 1). Taking into account that the concentration of NPsMagn in the soil does not change with depth, the possibility of absorption inside the roots and displacement with water flow, and not just adsorption onto sunflower roots as observed by Demangeat et al.,[54] must be considered to explain the root distribution of NPsMagn (Tab 1). Adsorption of NPsMagn onto roots is due to positive surface charges of NPsMagn which are more likely to adsorb and accumulate on root surfaces negatively charged.[70] On the other hand, depending on their size, NPs can penetrate the roots through the pores of the cell wall and then follow the apoplastic pathway to reach the vascular tissue. From the central cylinder (including the xylem and phloem), NPs can reach the aerial parts of plants by following the transpiration flow.[71] Based on the data in Fig. 5 and Tab 1, we cannot conclude on the presence of NPsMagn in the aerial tissues of sunflowers. However significant increase of Fe in whole aerial part and in stems of plants grown into NPsMagn-Pb media evidenced the possible

View Article Online
DOI: 10.1039/D2VA00283C

occurrence of a small amount of NPsMagn in sunflower stems. The translocation of NPsMagn in plants varies among studies. It can either be found in barley aerial parts and roots without cellular penetration[72] or be detected in pumpkin leaves and roots, in stems close to the roots as well as in the root surface.[73] On the contrary they were not translocated in ryegrass.[74]

As observed in Fig. 5B, the cumulative amount of Fe released in NPsMagn-Pb soil solution was eight time higher than in the soil solutions of the control soil. However, it is worth mentioning that the amount of Fe leached after 75 days only represented 0.04 % of Fe present in soil. These results corroborate those observed by Demangeat *et al*.[54] emphasizing that leaching had little effect on the mobility of NPsMagn in soil. An important increase on iron release in leachates took place from day 45 of the experiment in NPsMagn-Pb treatment. No pH or redox potential changes explaining this behavior before and after this release and the redox potential values are similar to other treatments. These patterns are not observed in leachates from treatments without plants, suggesting that plants play a role on iron release into the media. In fact, roots exudates (e.g. organic acids, sugars, amino acids, and proteins) or microbial activity (e.g. iron-reducing bacteria) may foster the dissolution of NPsMagn and Fe release into more bioavailable forms (such as those induced by the action of (phyto)siderophores).[75] In the context of IONPs environmental fate and ecotoxicity, our results highlights the low dispersion of NPsMagn into soil and the importance of the presence of a vegetation cover.

3.2.2. Chemical exchanges between plants, soil and soil solution

With the input of Pb in the soils, the amount of Pb was increased in plant stems and leaves (Fig. 5C) and in the leaching solutions (Fig. 5D). In all the aerial parts of the sunflowers, the Pb content tends to be higher when plants were grown in soil treated with NPsMagn-Pb than in those treated with Pb or µMagn-Pb (Fig. 5C). The Pb content in leaves increased significantly by 78 % and 102 % in sunflowers treated with NPsMagn compared to plants in the Pb and µMagn-Pb treatments, respectively. Furthermore, the Pb content in the stems is 6 to 9 times higher than in the leaves, with a maximum for the treatment with NPsMagn (22.93 mg kg^{-1}). Similar results have been observed in rice where Pb accumulate three times more in stems.[76] Results indicated that addition of NPsMagn, in appropriate amount to achieve an optimal removal of TEs, could effectively increase the accumulation capacity of Pb for the studied plant. Previous findings noticed an increased Pb accumulation capacity of *Kochia scoparia* in

View Article Online
DOI: 10.1039/D2VA00283C

nano zero valent iron amended soil up to a specific concentration of nanomaterials, then beyond this, Fe nanoparticle effect on Pb accumulation decreased.[77] They have found adverse effects of high concentrations of nano zero valent iron in soil on total Pb accumulation capacity of *K. scoparia*. In contrast, in another study, reduced accumulation of Pb in plant-soil system treated with compost added with maghemite nanoparticles was found.[30]

Remarkably, the leaching of Pb was decreased respectively by 37 % and 20 % in Pb-contaminated soil enriched with NPsMagn relative to soil without NPsMagn, both with and without sunflower plants (Fig. 5D). Within the same treatment, the presence of plants considerably affects the amount of Pb leached into the soil solution. Thus, lead content also decreases by 35 % and 50 % respectively in the presence of plants in the Pb and NPsMagn-Pb treatments compared to similar set-up without plants. Cover crop allowed to prevent TEs dispersion by water and wind erosion, as well as to reduce their mobility and bioavailability.[78] Phytostabilisation can happen depending of diverse processes (e.g. sorption, precipitation, complexation or valence reduction)[79] and is controlled by various components (such as, pH and redox potential, OM content, soil texture, soil structure or microorganisms).[80] TEs mainly accumulate at rhizosperic level and within roots tissues depending of several factors like roots exudates, microorganism's presence in the rhizosphere, the binding of TEs on the cell wall or with metal binding molecules or their accrual into vacuoles.[81]

In addition, IONPs have a high affinity for Pb depending on environmental conditions.[82] Thus, IONPs retain Pb in the soil and limit its dispersion in the soil solution as expected. In the treatments without plants, the soil pH is higher (pH 5.74 for cultivated soil and pH 6.45 for non-cultivated soil) which leads to a higher release of colloids to which Pb is bound.[83] Indeed, the impact of plants on leachate components can also be seen in Fig. 6 where the amount of dissolved organic carbon (DOC) is significantly higher by 92 % (Soil Pb) and 106 % (Soil NPsMagn-Pb) in leachates from set up without plants compared to their homologues with plants. Interestingly enough, even if the Pb proportion within leachates represent less than 0.2 % of total amount in soil, Pb concentration in leachates (e.g. 503 and 342 µg L^{-1} in cumulated leachates from respectively Pb and NPsMagn-Pb treatments, data not shown) and Pb retention by NPsMagn is relevant considering lead exposure through water sources.[84]

Moreover, it is worth to be noted that Pb adsorption by NPsMagn did not limit Pb uptake by the plant (Fig. 5C). At the rhizospheric level, Pb penetrates into roots via apoplastic pathway

View Article Online
DOI: 10.1039/D2VA00283C

or through Ca^{2+} permeable channels.[9] We can also hypothesize that binding of NPsMagn to the roots of sunflowers enhanced Pb uptake by plants by making rhizospheric Pb more bioavailable. Concerning roots exudates, Luo *et al.* showed that amino acids like alanine and proline could influence Pb uptake by *Sedum alfredii*.[85] Finally, even no growth improvement has been shown, plants treated with NPsMagn-Pb are doing as well as control or Pb-treated plants but with higher amounts of Pb in their aerial parts.

Furthermore, as discussed above, the amount of DOC is significantly higher in leachates from set up without plants compared to their homologues with plants. While in the presence of plants the NPsMagn-Pb treatment does not impact the DOC amount in leachates, DOC in leachates increased by 115 % and 167 % respectively for Pb and µMagn-Pb compared to control. To date, few studies have been conducted on the influence of OM on the surface reactions of IONPs. OM and IONPs interact mainly through adsorption of OM onto particle surfaces, and this adsorption has a significant impact on the adsorption of other ions and molecules.[86] Our results highlight that Pb seems to increase OM leaching and inversely, NPsMagn addition allowed to decrease OM loss in leachates. In addition, as discussed above for Pb leaching, the presence of plant within the experimental set-up seems to prevent OM leaching. Poirier *et al.* reviewed the link between roots characteristics and soil OM stabilization processes.[87] They identified several roots traits which participate to retain OM into soil: (i) accumulation in the rhizosphere of root molecules recalcitrant against decomposition (e.g. root suberin[88]), (ii) occlusion in soil aggregates, which limits access to microorganisms and enzymes, and (iii) interaction with soils minerals and metals (formation of stable organo-mineral associations).[89] Also, high roots length and density[90] are key factors for OM stabilization as it allows to entangle and aggregate of soil particles[91] and stimulate microbial activity by producing exudates that act as binding agent.[92]

3.3. Water stress response during interaction with NPsMagn-Pb

Research on NPs is growing, but few studies have investigated the relationships between NPs and rhizosphere as well as plant-water relations. However, the response of plants to water stress is a crucial element in their interactions with TEs. Recent studies on the application of NPs under water stress in plants show promising results.[93] Thus, we sought to evaluate the impact of NPsMagn on water relations in our cropping system in response to water stress

View Article Online
DOI: 10.1039/D2VA00283C

through different measurements. At each water stress period, all plants showed visual symptoms of water deficit but it was significantly less pronounced in sunflowers treated with NPsMagn. Different measurements have been performed to further investigate this observation. First, we determined soil water potential, which corresponds to a pressure measurement quantifying the energy level of the water molecules in a solution. The water potential of the NPsMagn treated soil was four times higher after a 3-days water stress than the water potential of control soil (Fig. 7A). It is likely that the addition of a nanoparticulate fraction (1 %) has modified the soil structure, as clay minerals do due to their high surface area, increasing the water reserve of the soil. Ajayi and Horn tested the addition of 2, 5 and 10 % of clay (bentonite) in fine sand which lead to an increase of water holding capacity.[94] It can be explained by the increasing internal surface area of the amended soil,[95] availability of binding site, and mineralogy of the clay material.[94,96] Thus, water can either be stored into soil macropores, attracted to the outer surfaces of clay minerals, or retained as intercalated water in spaces between clay layers.

In addition, we can expect that IONPs, that can bind to OM, could potentially promote soil water retention up to a certain threshold over a long-term effect. Results in Fig. 6 (section 3.2.2) confirm that DOC is more retained in soil in presence of NPsMagn. Those results support the hypothesis that NPsMagn could improve water retention in soil.[97]

In the search for easily measurable indicators of water stress, we made analyses of the effects of water stress periods on leaf angle. The evolution of the leaf angle according to field capacity (FC) or water deficiency (WD) periods shows that the plants of each treatment follow the same pattern except for those exposed to NPsMagn (Fig. 7B). Thus, leaf angle of control plants varies with increasing plant age in range of 106°±2 to 90°±4 during FC periods; and from 28°±2 to 74°±5 during the WD periods; that is to say a decrease in the angle from 73 % to 25 % for water stress periods starting at days 56th and 84th of plant culture, respectively. On the contrary, leaves angles of plants exposed to NPsMagn varies from 111°±5 to 105°±2 in FC and in range of 56°±3 to 107°±2 in WD, so that a significant reduction in leaf angles from only 49 % to 2 % for water stress periods starting at days 56th and 84th of plant culture, respectively. In addition, we have also evaluated the leaf relative water content (RWC) under water stress periods. As RWC reflects the balance between water supply to the leaf and transpiration rate, this is thus

View Article Online
DOI: 10.1039/D2VA00283C

an important indicator of water status in plants.[98] Interestingly, we determined that only in the presence of NPsMagn the leaf RWC is significantly higher compared to control (Fig. 7A).

Finally, in case of water stress, the determination of proline content is used as an indicator of stress in plants.[99] Here, no difference in proline content could be noted (Fig. 4). In their study on nano-maghemite, Martínez-Fernández *et al.* did not found any difference between treatment in RWC, leaves surface area or proline content in sunflower under water stress.[30] As in their study, we did not observe production of proline as a stress response marker, but rather with leaves angles and RWC and measurements on soil water potential. Even if some NPs have been shown to have a deleterious impact at the root level by mechanically disrupting cell membranes and walls, thus affecting water absorption by the roots,[100] in other cases NPs improve tolerance to water stress by affecting different physiological and biochemical mechanisms such as improvement of photosynthetic parameters, regulation of stomatal conductance, antioxidant activity, nutrient and water use efficiency or osmolyte content.[93] For instance, the application of different metal oxide NPs into soybean improved biomass reduction rate, RWC and drought tolerance index,[101] and IONPs treatment allowed to enhance biomass, photosynthesis efficiency, nutrient uptake and antioxidant enzymes content in *Oryza sativa.*[102]

Overall, our results show that NPsMagn seem to have a considerable impact on soil structure and water retention, which indirectly influences plant physiology. Further studies would be needed to describe these structural changes more precisely. In addition, gene expression analysis in plants treated with NPs under water stress conditions is a new avenue to explore because different studies show that application of NPs under water stress induces an increase in the expression of drought-responsive genes.[101,103] Thus, the improvement of drought tolerance could be mediated by triggering the expression of drought-related genes via NPs.

4. Conclusions

To conclude, even at high concentrations as those recommended for remediation, NPsMagn have little impact on the growth and on some physiological and biochemical responses of sunflower, and instead showed a protective effect against oxidative impact. Moreover, NPsMagn seem to enhance i) Pb availability and accumulation in plants, as higher amount of Pb has been measured in sunflower aerial parts, and ii) Pb stabilization within the soil, as

View Article Online
DOI: 10.1039/D2VA00283C

smaller amount of Pb has been determined in soil leachates. Likewise, Fe content was superior in plants treated with NPsMagn, and NPsMagn decreased the loss of soil dissolved organic matter and Pb transfer in leachates. Finally, here we show that plants treated with NPsMagn presented an improved water stress response and leaf water status, which could be in part explained by the enhanced retention of water in soils containing NPsMagn. All those results indicated that NPsMagn are promising materials for TEs remediation purposes, and are thus promising avenues of research, particularly for the agricultural sector, where water stress is one of the main causes of losses. However, further research is needed to understand the underlying mechanisms, especially at the molecular level. These data provide new answers where the knowledge about the environmental fate and toxicity of nanoparticles is still inadequate.

Author contributions

LM: conceptualization, methodology, validation, resources, formal analysis, investigation, data curation, writing – original draft, visualization. MBLC: methodology, validation, investigation. MP: conceptualization, methodology, validation, writing – review & editing, supervision, funding acquisition. FCH: conceptualization, methodology, validation, writing – review & editing, supervision, funding acquisition, project administration.

Conflicts of interest

Authors declare no conflicts of interest.

Acknowledgements

This work was supported by the SURFNANO project funded by the CNRS-INSU EC2CO program and the SynFeSol project funded by the Brittany Region (AAP TRANSFERT 2019). Through the support of the GeOHeLiS analytical platform of Rennes University, this publication is also supported by the European Union through the European Regional Development Fund (FEDER), the French Region of Brittany and Rennes Metropole. We also thank THEMIS plateform and Laura Fablet for their contribution to the TEM images acquisition as well as Pierrick Roperch

View Article Online
DOI: 10.1039/D2VA00283C

for magnetic susceptibility analyses. Léa Mounier was supported by a doctoral research grant from the University of Rennes 1–French Ministry of Higher Education and Research.

References

1 O. V. Singh, S. Labana, G. Pandey, R. Budhiraja and R. K. Jain, *Appl Microbiol Biotechnol*, 2003, **61**, 405–412.
2 G. S. Senesil, G. Baldassarre, N. Senesi and B. Radina, *Chemosphere*, 1999, **39**, 343–377.
3 A. Kushwaha, N. Hans, S. Kumar and R. Rani, *Ecotoxicology and Environmental Safety*, 2018, **147**, 1035–1045.
4 A. Kumar, A. Kumar, M. Cabral-Pinto, A. K. Chaturvedi, A. A. Shabnam, G. Subrahmanyam, R. Mondal, D. K. Gupta, S. K. Malyan, S. S. Kumar, S. A. Khan and K. K. Yadav, *International Journal of Environmental Research and Public Health*, 2020, **17**, 2179.
5 E. S. Perl, *International Journal of Phytoremediation*, 2020, **22**, 916–930.
6 E. Islam, X. Yang, T. Li, D. Liu, X. Jin and F. Meng, *Journal of Hazardous Materials*, 2007, **147**, 806–816.
7 P. Chauhan, A. B. Rajguru, M. Y. Dudhe and J. Mathur, *Environmental Technology & Innovation*, 2020, **18**, 100718.
8 F. Hadi, A. Bano and M. P. Fuller, *Chemosphere*, 2010, **80**, 457–462.
9 B. Pourrut, M. Shahid, C. Dumat, P. Winterton and E. Pinelli, in *Reviews of Environmental Contamination and Toxicology*, ed. D. M. Whitacre, New-York, Springer New York., 2011, vol. 213, pp. 113–136.
10 E. Keunen, T. Remans, S. Bohler, J. Vangronsveld and A. Cuypers, *International Journal of Molecular Sciences*, 2011, **12**, 6894–6918.
11 A. Kumar and M. N. V. Prasad, *Ecotoxicology and Environmental Safety*, 2018, **166**, 401–418.
12 N. Natasha, M. Shahid, S. Khalid, I. Bibi, M. A. Naeem, N. Niazi, F. Tack, J. Ippolito and J. Rinklebe, *Critical Reviews in Environmental Science and Technology*, 2021, **16**, 1–41.
13 G. Ali Mansoori, T. R. Bastami, A. Ahmadpour and Z. Eshaghi, in *Annual Review of Nano Research*, WORLD SCIENTIFIC, 2008, vol. **2**, pp. 439–493.
14 M. Rizwan, S. Ali, M. Z. ur Rehman, M. Riaz, M. Adrees, A. Hussain, Z. A. Zahir and J. Rinklebe, *Ecotoxicology and Environmental Safety*, 2021, **221**, 112437.
15 A. Latif, D. Sheng, K. Sun, Y. Si, M. Azeem, A. Abbas and M. Bilal, *Environmental Pollution*, 2020, **264**, 114728.
16 C. Claudio, E. di Iorio, Q. Liu, Z. Jiang and V. Barrón, *Journal of Nanoscience and Nanotechnology*, 2017, **17**, 4449–4460.
17 Z. Jiang, L. Lv, W. Zhang, Q. Du, B. Pan, L. Yang and Q. Zhang, *Water Research*, 2011, **45**, 2191–2198.
18 J. Chen, X. Qiu, Z. Fang, M. Yang, T. Pokeung, F. Gu, W. Cheng and B. Lan, *Chemical Engineering Journal*, 2012, **181–182**, 113–119.
19 L. Alidokht, A. R. Khataee, A. Reyhanitabar and S. Oustan, *Desalination*, 2011, **270**, 105–110.
20 H. K. Boparai, M. Joseph and D. M. O'Carroll, *Journal of Hazardous Materials*, 2011, **186**, 458–465.
21 H. Zhu, Y. Jia, X. Wu and H. Wang, *Journal of Hazardous Materials*, 2009, **172**, 1591–1596.
22 L. Liang, W. Yang, X. Guan, J. Li, Z. Xu, J. Wu, Y. Huang and X. Zhang, *Water Research*, 2013, **47**, 5846–5855.
23 X. Zhang, S. Lin, Z. Chen, M. Megharaj and R. Naidu, *Water Research*, 2011, **45**, 3481–3488.
24 M. Komárek, A. Vaněk and V. Ettler, *Environmental Pollution*, 2013, **172**, 9–22.
25 M. Auffan, J. Rose, O. Proux, D. Borschneck, A. Masion, P. Chaurand, J.-L. Hazemann, C. Chaneac, J.-P. Jolivet, M. R. Wiesner, A. Van Geen and J.-Y. Bottero, *Langmuir*, 2008, **24**, 3215–3222.
26 J. Tang, M. Myers, K. A. Bosnick and L. E. Brus, *J. Phys. Chem. B*, 2003, **107**, 7501–7506.
27 T. Borch, R. Kretzschmar, A. Kappler, P. V. Cappellen, M. Ginder-Vogel, A. Voegelin and K. Campbell, *Environ. Sci. Technol.*, 2010, **44**, 15–23.

28 S. U. Rahman, X. Wang, M. Shahzad, O. Bashir, Y. Li and H. Cheng, *Environmental Pollution*, 2022, **310**, 119916.
29 E. Demangeat, M. Pédrot, A. Dia, M. Bouhnik-Le-Coz, M. Davranche and F. Cabello-Hurtado, *Environmental Pollution*, 2020, **257**, 113626.
30 D. Martínez-Fernández, M. Vítková, M. P. Bernal and M. Komárek, *Water Air Soil Pollut*, 2015, **226**, 101.
31 M. Kah, N. Tufenkji and J. C. White, *Nat. Nanotechnol.*, 2019, **14**, 532–540.
32 C. O. Dimkpa, J. C. White, W. H. Elmer and J. Gardea-Torresdey, *J. Agric. Food Chem.*, 2017, **65**, 8552–8559.
33 X. Ma, J. Geiser-Lee, Y. Deng and A. Kolmakov, *Science of The Total Environment*, 2010, **408**, 3053–3061.
34 Fahad, A. Balouch, M. H. Agheem, S. A. Memon, A. R. Baloch, A. Tunio, Abdullah, A. H. Pato, M. S. Jagirani, P. Panah, A. A. Gabole and S. Qasim, *International Journal of Environmental Analytical Chemistry*, 2020, 1–12.
35 A. Konate, X. He, Z. Zhang, Y. Ma, P. Zhang, G. M. Alugongo and Y. Rui, *Sustainability*, 2017, **9**, 790.
36 M. Rui, C. Ma, Y. Hao, J. Guo, Y. Rui, X. Tang, Q. Zhao, X. Fan, Z. Zhang, T. Hou and S. Zhu, *Front. Plant Sci*, 2016, **7**, 815.
37 N. G. M. Palmqvist, G. A. Seisenbaeva, P. Svedlindh and V. G. Kessler, *Nanoscale Res Lett*, 2017, **12**, 631.
38 N. N. Nassar, *Journal of Hazardous Materials*, 2010, **184**, 538–546.
39 J. Cui, Q. Jin, Y. Li and F. Li, *Environ. Sci.: Nano*, 2019, **6**, 478–488.
40 P. Chauhan and J. Mathur, *Journal of Biological Sciences and Medecine*, 2018, **4**, 5–16.
41 F. Karam, R. Lahoud, R. Masaad, R. Kabalan, J. Breidi, C. Chalita and Y. Rouphael, *Agricultural Water Management*, 2007, **90**, 213–223.
42 E. Demangeat, M. Pédrot, A. Dia, M. Bouhnik-le-Coz, F. Grasset, K. Hanna, M. Kamagate and F. Cabello-Hurtado, *Environ. Sci.: Nano*, 2018, **5**, 992–1001.
43 R. Massart, *IEEE Trans. Magn.*, 1981, **17**, 1247–1248.
44 P. Jungcharoen, M. Pédrot, F. Choueikani, M. Pasturel, K. Hanna, F. Heberling, M. Tesfa and R. Marsac, *Environ. Sci.: Nano*, 2021, **8**, 2098–2107.
45 Journal Officiel République Française, 1998, https://www.legifrance.gouv.fr/jorf/id/JORFTEXT000000206637/ (accessed September 2020).
46 H. K. Lichtenthaler and A. R. Wellburn, *Biochemical Society Transactions*, 1983, **11**, 591–592.
47 E. W. Yemm, E. C. Cocking and R. E. Ricketts, *Analyst*, 1955, **80**, 209.
48 C. Magné and F. Larher, *Analytical Biochemistry*, 1992, **200**, 115–118.
49 Troll and J. Lindsley, *J Biol Chem*, 1955, 215–655.
50 D. M. Hodges, J. M. DeLong, C. F. Forney and R. K. Prange, *Planta*, 1999, **207**, 604–611.
51 M. M. Bradford, *Anal. Biochem.*, 1976, **72**, 248–254.
52 I. Cakmak and H. Marschner, *Plant Physiol*, 1992, **98**, 1222–1227.
53 C. N. Giannopolitis and S. K. Ries, *Plant Physiol.*, 1977, **59**, 309–314.
54 E. Demangeat, M. Pédrot, A. Dia, M. Bouhnik-Le-Coz, P. Roperch, G. Compaoré and F. Cabello-Hurtado, *Nanoscale Adv.*, 2021, **3**, 2017–2029.
55 M. Amde, J. Liu, Z.-Q. Tan and D. Bekana, *Environmental Pollution*, 2017, **230**, 250–267.
56 Z. Rengel, *Mechanisms of Environmental Stress Resistance in Plants*, CRC Press, 1997.
57 P. Madejon, J. Murillo, T. Maranon, F. Cabrera and M. Soriano, *The Science of The Total Environment*, 2003, **307**, 239–257.
58 D. K. Tripathi, Shweta, S. Singh, S. Singh, R. Pandey, V. P. Singh, N. C. Sharma, S. M. Prasad, N. K. Dubey and D. K. Chauhan, *Plant Physiology and Biochemistry*, 2017, **110**, 2–12.
59 M. Ursache-Oprisan, E. Focanici, D. Creanga and O. Caltun, *African Journal of Biotechnology*, 2011, **36**, 7092–7098.
60 Y. Wang, S. Wang, M. Xu, L. Xiao, Z. Dai and J. Li, *Environmental Pollution*, 2019, **249**, 1011–1018.
61 M. H. Ghafariyan, M. J. Malakouti, M. R. Dadpour, P. Stroeve and M. Mahmoudi, *Environ. Sci. Technol.*, 2013, 10645–10652.

62 Z. Zahra, N. Waseem, R. Zahra, H. Lee, M. A. Badshah, A. Mehmood, H.-K. Choi and M. Arshad, *Agric. Food Chem.*, 2017, **65**, 5598–5606.
63 S. Silva, T. P. Ribeiro, C. Santos, D. C. G. A. Pinto and A. M. S. Silva, *Journal of Hazardous Materials*, 2020, **399**, 122982.
64 Y. Wang, F. Jiang, C. Ma, Y. Rui, D. C. W. Tsang and B. Xing, *Journal of Environmental Management*, 2019, **241**, 319–327.
65 M. F. Iannone, M. D. Groppa, M. E. de Sousa, M. B. Fernández van Raap and M. P. Benavides, *Environmental and Experimental Botany*, 2016, **131**, 77–88.
66 T. Abedi and H. Pakniyat, *Czech J. Genet. Plant Breed*, 2010, **46**, 27–34.
67 J. Patykowski and J. Kołodziejek, *Pol. J. Environ. Stud.*, 2016, **25**, 725–732.
68 T. M. Hildebrandt, *Plant Mol Biol*, 2018, **98**, 121–135.
69 M. Al-Sid-Cheikh, M. Pédrot, A. Dia, M. Davranche, L. Jeanneau, P. Petitjean, M. Bouhnik-Le Coz, M.-A. Cormier and F. Grasset, *Environ. Sci.: Nano*, 2019, **6**, 3049–3059.
70 J. Lv, P. Christie and S. Zhang, *Environ. Sci.: Nano*, 2019, **6**, 41–59.
71 A. Pérez-de-Luque, *Frontiers in Environmental Science,* 2017, **5**, 5-12.
72 H. Tombuloglu, Y. Slimani, G. Tombuloglu, M. Almessiere and A. Baykal, *Chemosphere*, 2019, **226**, 110–122.
73 H. Zhu, J. Han, J. Q. Xiao and Y. Jin, *J. Environ. Monit.*, 2008, **10**, 685–784.
74 H. Wang, X. Kou, Z. Pei, J. Q. Xiao, X. Shan and B. Xing, *Nanotoxicology*, 2011, **5**, 30–42.
75 S. Bastani, R. Hajiboland, M. Khatamian and M. Saket-Oskoui, *J. Soil Sci. Plant Nutr.*, 2018, **18**, 524–541.
76 U. Ashraf, M. H.-R. Mahmood, S. Hussain, F. Abbas, S. A. Anjum and X. Tang, *Chemosphere*, 2020, **248**, 126003.
77 A. Daryabeigi Zand and A. Mikaeili Tabrizi, *Environmental Engineering Research*, 2020, **26**, 200227–0.
78 N. S. Bolan, J. H. Park, B. Robinson, R. Naidu and K. Y. Huh, in *Advances in Agronomy*, Elsevier, 2011, vol. **112**, pp. 145–204.
79 M. Ghosh, *Appl Ecol Env Res*, 2005, **3**, 1–18.
80 V. Chaignon, D. Di Malta and P. Hinsinger, *New Phytologist*, 2002, **154**, 121–130.
81 A. M. Shackira and J. T. Puthur, in *Plant-Metal Interactions*, eds. S. Srivastava, A. K. Srivastava and P. Suprasanna, Springer International Publishing, Cham, 2019, pp. 263–282.
82 J.-F. Liu, Z.-S. Zhao and G.-B. Jiang, *Environmental Science & Technology*, 2008, **42**, 6949–6954.
83 M. Pédrot, A. Dia and M. Davranche, *Journal of Colloid and Interface Science*, 2009, **339**, 390–403.
84 P. Jarvis and J. Fawell, *Current Opinion in Environmental Science & Health*, 2021, **20**, 100239.
85 Q. Luo, S. Wang, L. Sun and H. Wang, *Sci Rep*, 2017, **7**, 39878.
86 A. M. Vindedahl, J. H. Strehlau, W. A. Arnold and R. L. Penn, *Environ. Sci.: Nano*, 2016, **3**, 494–505.
87 V. Poirier, C. Roumet and A. D. Munson, *Soil Biology and Biochemistry*, 2018, **120**, 246–259.
88 A. Andreetta, M.-F. Dignac and S. Carnicelli, *Biogeochemistry*, 2013, **112**, 41–58.
89 F. Watteau, G. Villemin, G. Burtin and L. Jocteur-Monrozier, *European Journal of Soil Science*, 2006, **57**, 247–257.
90 G. Bodner, D. Leitner and H.-P. Kaul, *Plant Soil*, 2014, **380**, 133–151.
91 D. A. Angers and J. Caron, *Biogeochemistry*, 1998, **42**, 55–72.
92 I. J. Gould, J. N. Quinton, A. Weigelt, G. B. De Deyn and R. D. Bardgett, *Ecology Letters*, 2016, **19**, 1140–1149.
93 N. Kandhol, M. Jain and D. K. Tripathi, *Physiologia Plantarum*, 2022, **174**, e13665.
94 A. E. Ajayi and R. Horn, *International Agrophysics*, 2016, **30**, 391-399.
95 P. Hartmann, H. Fleige and R. Horn, *Geoderma*, 2009, **150**, 188–195.
96 A. E. Ajayi, D. Holthusen and R. Horn, *Soil and Tillage Research*, 2016, **155**, 166–175.
97 R. Lal, *Agronomy Journal*, 2020, **112**, 3265–3277.
98 D. Soltys-Kalina, J. Plich, D. Strzelczyk-Żyta, J. Śliwka and W. Marczewski, *Breed. Sci.*, 2016, **66**, 328–331.
99 N. Verbruggen and C. Hermans, *Amino Acids*, 2008, **35**, 753–759.

View Article Online
DOI: 10.1039/D2VA00283C

100 S. J. Klaine, P. J. J. Alvarez, G. E. Batley, T. F. Fernandes, R. D. Handy, D. Y. Lyon, S. Mahendra, M. J. McLaughlin and J. R. Lead, *Environmental Toxicology and Chemistry*, 2008, **27**, 1825–1851.

101 T. M. Linh, N. C. Mai, P. T. Hoe, L. Q. Lien, N. K. Ban, L. T. T. Hien, N. H. Chau and N. T. Van, *Journal of Nanomaterials*, 2020, **2020**, e4056563.

102 T. Ahmed, M. Noman, N. Manzoor, M. Shahid, M. Abdullah, L. Ali, G. Wang, A. Hashem, A.-B. F. Al-Arjani, A. A. Alqarawi, E. F. Abd_Allah and B. Li, *Ecotoxicology and Environmental Safety*, 2021, **209**, 111829.

103 Y.-T. Du, M.-J. Zhao, C.-T. Wang, Y. Gao, Y.-X. Wang, Y.-W. Liu, M. Chen, J. Chen, Y.-B. Zhou, Z.-S. Xu and Y.-Z. Ma, *BMC Plant Biology*, 2018, **18**, 320.

Figures

View Article Online
DOI: 10.1039/D2VA00283C

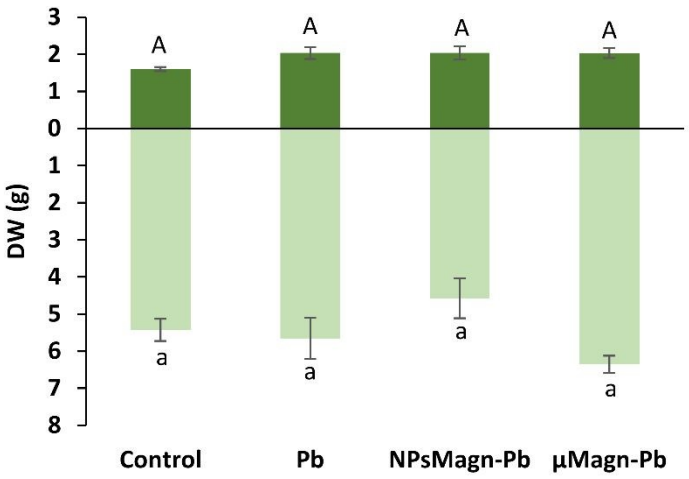

Fig. 1 Dry weight (g) of leaves (dark green) and stems (light green) of sunflower plants measured after 90 days of growth on control soil or containing Pb, NPsMagn-Pb or µMagn-Pb. Data represent the mean ± SEM (n= 6). Different letters indicate significant differences between treatments for each plant organ ($p < 0.05$).

View Article Online
DOI: 10.1039/D2VA00283C

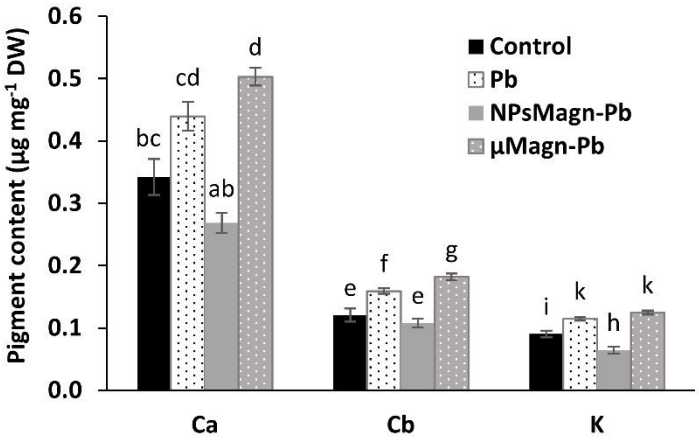

Fig. 2 Pigment content (µg mg^{-1} DW) measured in the leaves of sunflower plants after 90 days of growth on control soil or containing Pb, NPsMagn-Pb or µMagn-Pb. Data represent the mean ± SEM (n=6) of the pigment content measured in the leaves of sunflowers grown for 90 days in the different studied soils. Different letters above the bars indicate significant differences ($p < 0.05$).

View Article Online
DOI: 10.1039/D2VA00283C

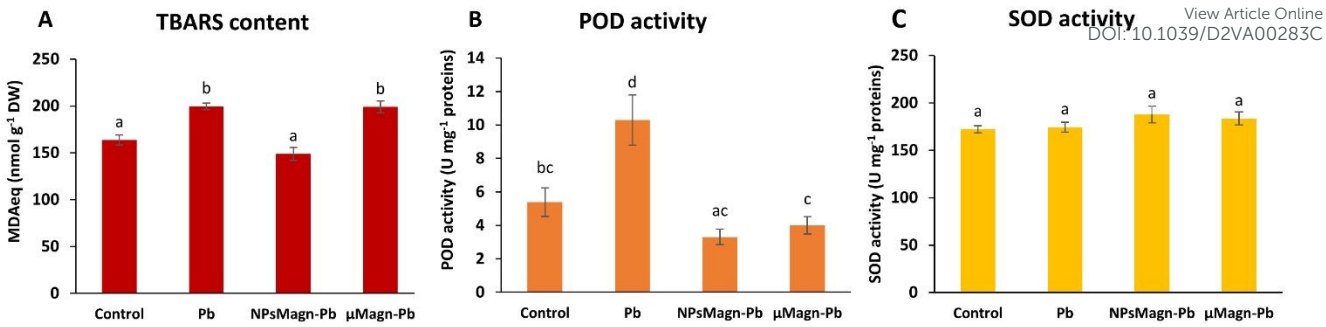

Fig. 3 Lipid peroxidation and antioxidant activities measured in the leaves of sunflower plants after 90 days of growth on control soil or containing Pb, NPsMagn-Pb or µMagn-Pb. (A) TBARS content (nmol MDAeq per g DW); (B) POD activity (U mg^{-1} protein); (C) SOD activity (U mg^{-1} protein). Data represent the mean ± SEM (n=6). Different letters above the bars indicate significant differences ($p < 0.05$).

View Article Online
DOI: 10.1039/D2VA00283C

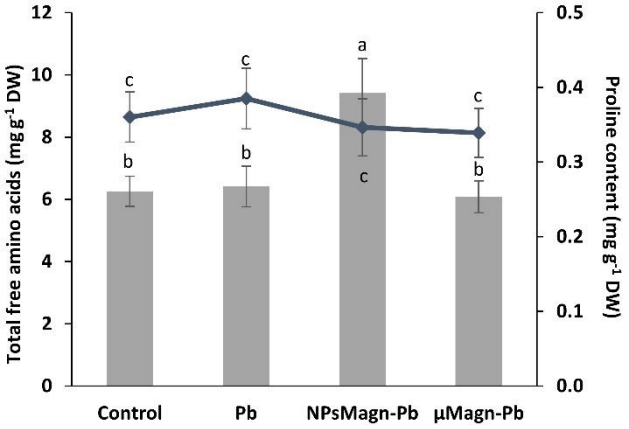

Fig. 4 Total free amino acids ($mg_{eq\ leucine}\ g^{-1}$ DW) (histogram) and proline content (mg g^{-1} DW) (curve) measured in the leaves of sunflower plants after 90 days of growth on control soil or containing Pb, NPsMagn-Pb or µMagn-Pb. Data represent the mean ± SEM (n=6). Different letters above the bars indicate significant differences ($p < 0.05$).

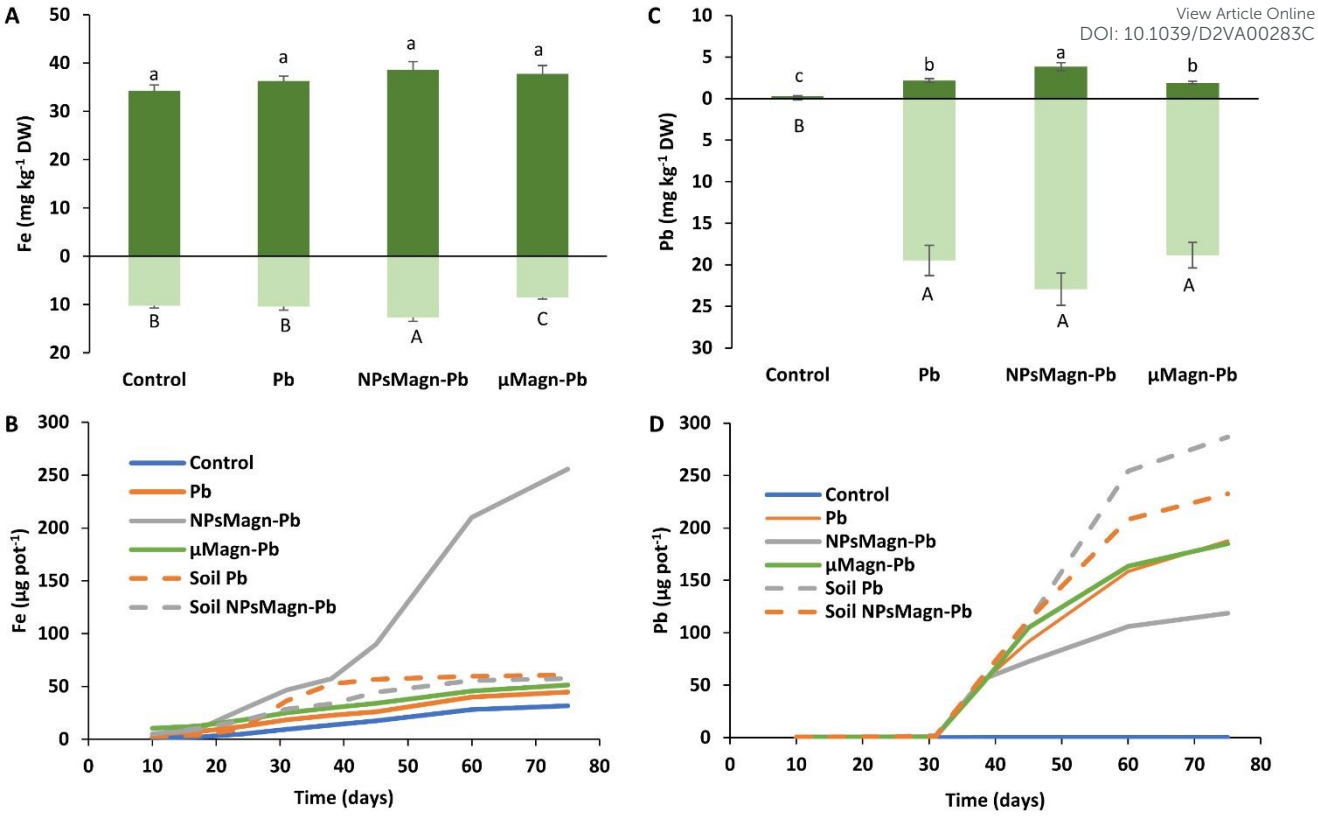

Fig. 5 Iron (A) and lead (C) concentrations (mg kg^{-1} DW) in leaves (dark green) and stems (light green) measured by ICP-MS after 90 days of growth in the different studied soils. Data represent the mean ± SEM (n=6). Different letters above or below the bars indicate significant differences between treatments for each plant organ ($p < 0.05$). Cumulative amounts of iron (B) and lead (D) leached (µg pot^{-1}) over the experimentation (day 10 to day 75) measured by ICP-MS. Dotted lines represent treatments without plant. Data represent the mean (n=2).

View Article Online
DOI: 10.1039/D2VA00283C

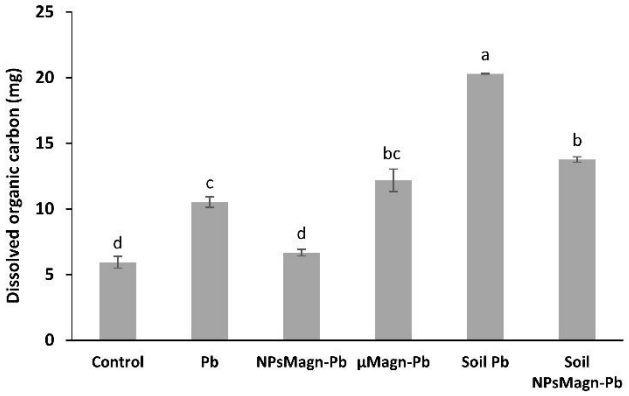

Fig. 6 Total amount of dissolved organic carbon leached over the experiment (mg). Leachates were filtrated at 0.2µm with syringe filters to dissociate the particulate from the dissolved phase. Data represent the mean ± SEM (n=6). Different letters above the bars indicate significant differences ($p < 0.05$).

View Article Online
DOI: 10.1039/D2VA00283C

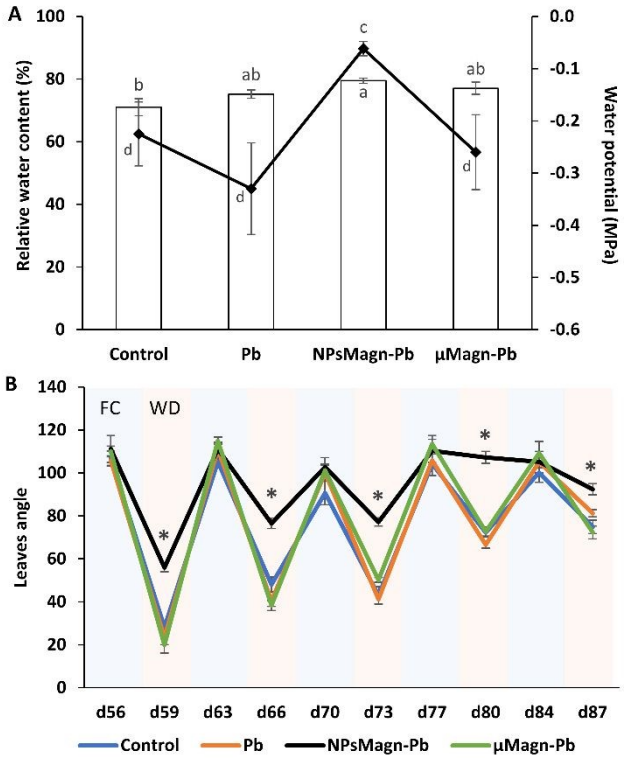

Fig. 7 Stress water response measured during and after 90 days of growth on control soil or containing Pb, NPsMagn-Pb or µMagn-Pb. (A) Water potential (histogram) of the different studied soils measured by WP4C dew meter point after plants harvest and relative water content (%) (curve) measured in the leaves of sunflower plants after 90 days of growth. (B) Leaves angle measured at different times of culture (FC = field capacity, pale blue; WD = water deficiency, pale pink). Measures correspond to the angle between the abaxial face of the leaf and the petiole. Data represent the mean ± SEM (n=6 or 12 for leaves angle). Different letters above the bars indicate significant differences ($p < 0.05$). An asterisk indicates significant difference with control ($p < 0.05$).

View Article Online
DOI: 10.1039/D2VA00283C

Table 1 Magnetite nanoparticles concentration (mg kg^{-1}) in sunflower roots and aerial parts, and in the soil samples, calculated from magnetic susceptibility measurements. Soil samples and sunflower plants were harvested after 90 days of exposure to NPsMagn-Pb. The quantification limit (QL) was determined at 40 mg kg^{-1}. Data represent the mean ± SEM (n=6). Different letters above indicate significant differences among plant or soil parts ($p < 0.05$).

		NPsMagn-Pb
Leaves	L1	<QL
	L2	<QL
	L3	<QL
Stem	T1	<QL
	T2	<QL
	T3	<QL
Roots	R1	3319 ± 493 [a]
	R2	1895 ± 435 [b]
	R3	1074 ± 164 [b]
Soil	S1	8171 ± 267 [a]
	S2	8587 ± 296 [a]
	S3	8202 ± 383 [a]